

## Mössbauer studies of electric hyperfine interactions in $^{234}\text{U}$ , $^{236}\text{U}$ , $^{238}\text{U}$ †

Joyce A. Monard\*, Paul G. Huray, and John O. Thomson

Department of Physics, The University of Tennessee, Knoxville, Tennessee 37916

Oak Ridge National Laboratory, Oak Ridge, Tennessee 37830

(Received 16 June 1972)

The nuclear  $\gamma$  resonances for  $^{234}\text{U}$ ,  $^{236}\text{U}$ , and  $^{238}\text{U}$  in the compound  $(\text{UO}_2)\text{Rb}(\text{NO}_3)_3$  have been observed using sources of  $\text{PuO}_2$  and  $\text{PuAl}_4$ . Nuclear deformations of the U isotopes are observed to change through the ratios of the electric quadrupole moments. Using previous  $B(E2)$  measurements the electric field gradient at the uranium site has been calculated for this compound from our data. The isomer shift of  $^{234}\text{U}$  has been measured for  $(\text{UO}_2)\text{Rb}(\text{NO}_3)_3$  and for the two sources  $\text{PuO}_2$  and  $\text{PuAl}_4$ . Calculations of electronic charge density changes at uranium nuclei between source and absorbers give a fractional decrease in the rms nuclear radius in the transition from the ground to the excited state of  $(\delta \langle r_n^2 \rangle / \langle r_n^2 \rangle)_{234\text{U}} = (-12.2 \pm 5.9) \times 10^{-6}$ .

### I. INTRODUCTION

The  $\gamma$  transition from the  $2^+$  excited state to the  $0^+$  ground state in the even-even isotopes of the actinide elements has been recognized for several years as a Mössbauer resonance<sup>1,2</sup> and consequently a tool for the study of their nuclear and solid-state properties. The experiments prove difficult for several reasons: Both sources and absorbers are radioactive; the high isotopic purities required for successful experiments are expensive and scarce; and the heavy elements are extremely toxic in general. Moreover, the large internal-conversion coefficients of the resonant  $\gamma$  rays seriously decrease the source  $\gamma$ -ray intensity and the resonant-absorption cross section. Finally, nuclear recoil and/or radiation damage in the source may affect the Mössbauer resonance whether the excited state is reached by Coulomb excitation<sup>3,4</sup> or by  $\alpha$  decay.<sup>5-8</sup>

We have obtained Mössbauer spectra for three uranium isotopes using radioactive decay from plutonium parents. The  $\alpha$  decays of  $^{238}\text{Pu}$ ,  $^{240}\text{Pu}$ , and  $^{242}\text{Pu}$  populate the  $2^+$  rotational states of  $^{234}\text{U}$ ,  $^{236}\text{U}$ , and  $^{238}\text{U}$ , respectively, about 25% of the time. The subsequent  $E2$  transition to the  $0^+$  ground state occurs with the emission of an  $\sim 45$ -keV  $\gamma$  ray about once in every 650 events. Comparative nuclear parameters of all three isotopes are tabulated in Refs. 9 and 10.

### II. EXPERIMENTAL

One of the source materials used in this study was the compound  $\text{PuO}_2$  which is cubic,<sup>11</sup> and nonmagnetic,<sup>12</sup> and thus should produce an unsplit  $\gamma$ -ray emission line.<sup>7,8</sup> Both  $\text{PuO}_2$  and  $\text{UO}_2$  exhibit the face-centered cubic fluorite ( $\text{CaF}_2$ ) structure.<sup>13</sup> There are four plutonium and eight oxygen atoms per unit cell. The oxygen atoms are in a simple cubic packing within the unit cell which is bounded by plutonium atoms at the cell corners and face-

centered positions.

Another  $\gamma$ -source material,  $\text{PuAl}_4$ , was also used in this study. This intermetallic compound exhibits the body-centered orthorhombic  $\text{UAl}_4$  structure<sup>14</sup> and has four formula units per unit cell. The lattice constants for  $\text{PuAl}_4$ <sup>15</sup> are within experimental error equal to those for  $\text{UAl}_4$ .<sup>14</sup> Although the Pu site in this compound does not possess cubic symmetry, Gregory *et al.*<sup>16</sup> have shown that  $^{243}\text{PuAl}_4$  sources produce an even narrower line than  $^{243}\text{PuO}_2$  sources for the Mössbauer resonance in  $^{243}\text{Am}$ .

Typically about 0.6 g of finely powdered source material was doubly encapsulated in aluminum containers with 0.01-in.-thick windows.<sup>17</sup> A 0.030-in.-thick beryllium plate was placed between the two containers to provide added strength. The diameter of the inner container was approximately 1 in. and thus gave sources with a thickness of about 90 mg/cm<sup>2</sup> of plutonium for each source.

As an absorber material we chose the nonmagnetic uranyl rubidium nitrate  $[(\text{UO}_2)\text{Rb}(\text{NO}_3)_3]$  which is known to have a large electric field gradient at the uranium site.<sup>18-20</sup> The chemical oxidation state of the U ion in this compound is nominally +6 relative to the free ion. The crystal is a member of the hexagonal system (rhombohedral division). The primitive rhombohedron contains two stoichiometric molecules.<sup>21</sup> X-ray intensity data show that both uranium and rubidium lie on body-centered rhombohedral sublattices and that the origins of the two sublattices are separated by  $\frac{1}{2}c$  along the unique axis. The linear uranyl groups all lie parallel to the  $c$  axis of the crystal, each surrounded by three nitrate groups in the equatorial plane. Recent Raman and infrared spectroscopic studies<sup>22</sup> confirm that the uranyl ion is linear, and x-ray studies<sup>23</sup> find the uranium-oxygen bond length in the uranyl ion to be 1.78 Å. This bond length is much smaller than the distance of 2.72 Å between the uranium atom and its next-nearest neighbors, the six oxygen atoms in the nitrate groups. The

nitrate are thus thought to have little effect on the strong uranyl bonding. A schematic of the molecule is shown in Fig. 1. Due to the high degree of symmetry of the molecule, the antisymmetry term of the quadrupole interaction has been neglected in the data analysis.

About 1.3 g of finely powdered  $(\text{UO}_2)\text{Rb}(\text{NO}_3)_3$  was combined with about 2.0 g of finely powdered lucite and pressed into a disk of 1.375-in. diameter. The absorber thickness was thus on the order of  $60 \text{ mg/cm}^2$  of uranium. Isotopic purities of the  $^{242}\text{Pu}$ ,  $^{240}\text{Pu}$ , and  $^{238}\text{Pu}$  sources and  $^{238}\text{U}$ ,  $^{236}\text{U}$ , and  $^{234}\text{U}$  absorbers were 99.99%, 98.30%, and 79.53%, and 99.98%, 99.68%, and 86.61%, respectively. These were the best available from the Atomic Energy Commission at that time.

Mössbauer measurements were made at  $4.2^\circ\text{K}$  in a metal Dewar with thin beryllium windows.  $\gamma$  rays for the 45-keV resonance were detected by a  $7\text{-cm}^2$  Ge(Li) detector with a resolution of 2.3 keV at 60 keV. A sine-wave electromechanical transducer driven at resonance ( $\sim 15 \text{ Hz}$ ) with a feedback circuit was used to Doppler shift the absorber with respect to the source. The Mössbauer spectra were collected in a 1024-channel analyzer operating synchronously with the absorber in the multiscale mode. At the high velocities required,

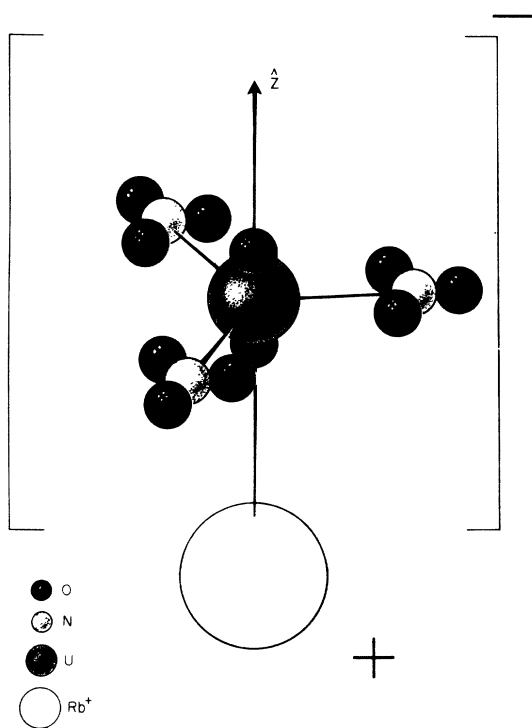


FIG. 1. Structure of the uranyl rubidium nitrate molecule. The three nitrate groups are shown lying in a plane perpendicular to the collinear O-U-O entity.

the velocity scale was determined by a specially constructed pickup coil surrounding a magnet moving with the absorber. The coil was designed to give an output voltage both linear in velocity and insensitive to sidewise motion of the transducer to one part in  $10^5$  and was calibrated using an Fe-metal Mössbauer spectrum. The pickup voltage was fed to a voltage-to-frequency converter and the resulting pulses were multiscaled in the second bank of 1024 channels in the multichannel analyzer which were stepped synchronously with the first. Thus a check on the quality of the velocity waveform was obtained. For the purpose of accurately determining the zero of velocity in isomer-shift measurements, a Co-in-Cu source was attached to the top end of the transducer rod which moved the uranium absorber. In this way room-temperature Mössbauer spectra for an unsplit stainless-steel absorber could be collected simultaneously at the top of the Dewar system. These data were stored in the second set of 1024 channels for the case of isomer-shift runs and provided a reference point for the velocity of  $-0.375 \pm 0.010 \text{ mm/sec}$ . Although it is possible for the sinusoidal variation of velocity at one end of a transducer to lag or lead the sinusoidal variation at the driven end of a transducer (the top end in our case), an error in an isomer-shift determination brought about by this effect will to first order be canceled when one averages the upward-swinging velocity spectrum with the downward-swinging spectrum. In all spectra reported here, this effect was considered and was consistent with a lag of  $\sim 1$  channel out of 1024.

### III. HYPERFINE INTERACTIONS

Mössbauer hyperfine spectra for nonmagnetic absorbers and single-line sources can be described by a spin Hamiltonian for purely electric multipole interactions.<sup>24,25</sup> The electric monopole term leads to different shifts of the energy of both the excited and ground states of a nucleus involved in the emission or absorption of a  $\gamma$  ray and in first-order perturbation theory is given as

$$E = \int_0^r \int_0^{2\pi} \int_0^a \rho_n(\vec{r}_n) \left[ \int_0^r \int_0^{2\pi} \int_0^{r_n} \rho_e(\vec{r}_e) \times \left( \frac{1}{r_n} - \frac{1}{r_e} \right) d\tau_e \right] d\tau_n, \quad (1)$$

where  $\rho_e(\vec{r}_e)$  is the electronic charge-density distribution,  $\rho_n(\vec{r}_n)$  is the nuclear charge-density distribution, and  $a$  is the maximum extent of the nuclear charge. Usually one evaluates these integrals by assuming that  $\rho_e(\vec{r}_e)$  is constant over the dimensions of the nucleus (i. e., for  $|\vec{r}_e| < a$ ) and that  $\rho_n(\vec{r}_n)$  is a spherically symmetric total charge  $Z|e|$  distributed over the volume of a sphere of radius  $R_0 = a$ . Under this set of assumptions the electric monopole

term [Eq. (1)] leads to a shift of the excited and ground states ( $E^*$  and  $E$ ) of both the source and absorber nuclei and results in an energy shift  $\delta_{IS} = (E^* - E)_{\text{source}} - (E^* - E)_{\text{absorber}}$  of  $\gamma$  rays in a resonant process. This energy shift (the isomer shift) is then expressed as

$$\delta_{IS} = \frac{2}{3} \pi |e| \Delta |\psi(0)|^2 \delta \langle r_n^2 \rangle, \quad (2)$$

where  $\Delta |\psi(0)|^2 = \rho_e^s(0) - \rho_e^A(0) = |\psi(0)|_{\text{source}}^2 - |\psi(0)|_{\text{absorber}}^2$  and  $\delta \langle r_n^2 \rangle = (\langle r_n^2 \rangle^* - \langle r_n^2 \rangle)$ . Here  $\langle r_n^2 \rangle = \int_0^a \rho_n(r_n) r_n^2 dr_n$ . Inasmuch as Ford *et al.*<sup>28</sup> have shown that this nucleus is highly distorted and since the relativistic electron charge density falls off significantly within the U nucleus<sup>27</sup> ( $\sim 18\%$  between  $r_n = 0$  and  $r_n = a$ ), the validity of the above set of assumptions should be examined.

Bohr and Weisskopf<sup>27</sup> have suggested that the major and minor components of the relativistic electron wave-function interior to a uniformly charged sphere of radius  $R_0$  leads to a radial dependence of the electron charge density for  $s$  electrons which is given by

$$\rho_e(r_e) = - |e| |\psi(0)|^2 \times \left[ 1 - \alpha \left( \frac{r_e}{R_0} \right)^2 - \gamma \left( \frac{r_e}{R_0} \right)^4 - \dots \right], \quad (3)$$

where  $\alpha = \frac{1}{2} \left( \frac{1}{137} Z \right)^2$  and  $\gamma = -\frac{3}{32} \left( \alpha - \frac{8}{5} \alpha^2 \right)$ .

For the case of U ( $Z = 92$ ),  $\alpha = 0.225$  and  $\gamma = -0.041$ , and we may conveniently approximate the electron charge-density fall off by retaining only terms through  $(r_e/R_0)^4$  in Eq. (3). With this function and Eq. (1) the isomer shift is given by

$$\delta_{IS} = \frac{2}{3} \pi |e| \Delta |\psi(0)|^2 \times \delta \langle r_n^2 [1 - \alpha \frac{3}{10} (r_n/R_0)^2 - \gamma \frac{1}{7} (r_n/R_0)^4] \rangle, \quad (4)$$

where

$$\Delta |\psi(0)|^2 = \rho_e^s(0) - \rho_e^A(0) = |\psi(0)|_{\text{source}}^2 - |\psi(0)|_{\text{absorber}}^2,$$

as before, and  $\delta \langle \dots \rangle = (\langle \dots \rangle^* - \langle \dots \rangle)$  as in Eq. (2). In contrast to Eq. (2) the  $\langle \dots \rangle$  is given by

$$\langle \dots \rangle = \int_0^a \rho_n(r_n) [1 - \alpha \frac{3}{10} (r_n/R_0)^2 - \gamma \frac{1}{7} (r_n/R_0)^4] r_n^2 dr_n.$$

In order to compare the departure of Eq. (4) from the value given in Eq. (2) we have computed the integral involved in  $\langle \dots \rangle$  in both expressions under the further assumption that the nuclear charge  $Z|e|$  is spread uniformly over the volume of an axially symmetric object of revolution whose radius is given by  $R = R_0 [1 + \beta_2 Y_{20}(\theta) + \beta_4 Y_{40}(\theta) + \dots]$ . The  $Y_{lm}(\theta)$  are the normalized spherical harmonics. In the evaluation of these integrals we have required a constant nuclear volume in order that only the ef-

fects of nuclear distortion play a role in the result. Figure 2 shows the results of these computations for several possible values of  $\beta_2$  and  $\beta_4$ . In the results shown in this figure  $\beta_6, \beta_8, \dots$  were all set = 0. In a separate calculation with  $\beta_6 \neq 0$ , the variation of this ratio with  $\beta_6$  was of much less significance than with either of the  $\beta_2$  or  $\beta_4$  variations. Calculations of Nilsson *et al.*<sup>28</sup> would suggest values of  $|\beta_6| < 0.02$  so that the effect of this term appears to be negligible.

If one chooses the values  $\beta_2 = 0.223 \pm 0.006$  and  $\beta_4 = 0.123 \pm 0.022$ , as measured by Bemis *et al.*<sup>29</sup> for the  $^{234}\text{U}$  nucleus, the resulting departure of Eq. (4) from the value given in Eq. (2) is seen from the single data point of Fig. 2 to be less than 2% and we shall neglect it in the following discussion.

The quadrupole term of the electronic-nuclear interaction leads to a splitting of the nuclear states and is described by the Hamiltonian

$$\hat{H} = \frac{eqQ}{4I(2I-1)} [(3\hat{I}_z^2 - \hat{I}^2) + \frac{1}{2}\eta(\hat{I}_+^2 + \hat{I}_-^2)], \quad (5)$$

where  $eQ$  is the spectroscopic nuclear quadrupole moment of the  $I=2$  excited state,  $q = -\partial E_z / \partial z$  is the negative of the electric field gradient at the uranium nucleus in the absorber,  $\hat{I}_z, \hat{I}_+, \hat{I}_-$  are the usual angular momentum operators; and

$$\eta = \left( \frac{\partial E_x}{\partial x} - \frac{\partial E_y}{\partial y} \right) / \frac{\partial E_z}{\partial z}$$

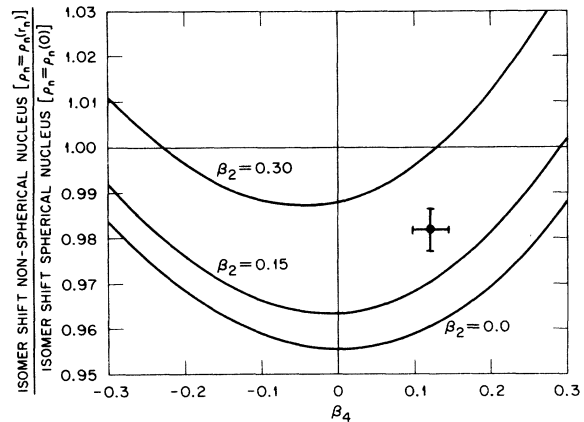


FIG. 2. Results of calculations of the ratio of the isomer shift for U nuclei obtained through two techniques: (a) a contact interaction which accounts for a uniformly distributed nuclear charge over a distorted nuclear shape and a radially dependent relativistic electron wave function; (b) a contact interaction obtained for the more idealized case of a spherical nuclear charge density and a flat relativistic electronic wave function. As seen from the figure, no nuclear distortion ( $\beta_2 = \beta_4 = 0$ ) produces a 4.5% difference in the isomer shift calculations due to radial electron charge-density falloff.

is the asymmetry parameter. Noting that the O-U-O bond in  $(\text{UO}_2)_2\text{Rb}(\text{NO}_3)_3$  is linear<sup>30-32</sup> and axially symmetric, we have chosen the quantization axis along this bond axis and therefore assumed that the  $\eta$  term is negligible. Thus the  $2^+$  state splits into three degenerate substates positioned at the energies  $E_{+2} = \frac{2}{3}eqQ$ ,  $E_{+1} = -\frac{1}{3}eqQ$ ,  $E_0 = -\frac{2}{3}eqQ$  relative to the unsplit energy. The resulting three-line Mössbauer spectrum should have an energy splitting ratio of 3:1 and relative line intensities of 2:2:1.

We have investigated the importance of a hexadecapole interaction in the spin Hamiltonian and (excluding an unreasonably large Sternheimer factor) find it to be beyond the limit of accuracy of our measurement.

#### IV. RESULTS

The uranium Mössbauer absorption spectrum for  $^{234}\text{U}$  in  $(\text{UO}_2)_2\text{Rb}(\text{NO}_3)_3$  at 4.2°K is shown in Fig. 3. These data are similar to all the uranium measurements to be presented with respect to the number of measured points and the quality of the fit of a theoretical line shape to the data. However for  $^{236}\text{U}$  and  $^{238}\text{U}$  lower specific activity of the parent Pu isotopes resulted in fewer accumulated counts and hence reduced the accuracy with which the hyperfine interactions could be determined. The solid curve in Fig. 3 is a least-squares fit of the full transmission integral to a pure symmetric electric quadrupole interaction ( $\eta = 0$ ). The line positions have been constrained to the theoretical splitting

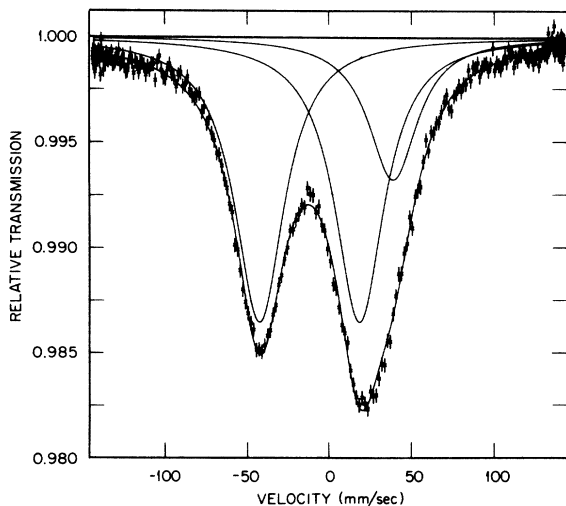


FIG. 3. Mössbauer spectrum of  $^{234}\text{U}$  in  $(\text{UO}_2)_2\text{Rb}(\text{NO}_3)_3$  following  $\alpha$  decay of  $^{238}\text{Pu}$  in  $\text{PuAl}_4$  at 4.2°K. The solid lines are a theoretical fit to the data using the full transmission integral. The positions and intensity ratios were constrained to represent the degenerate levels of a pure symmetric electric quadrupole interaction as described in the text.

ratio of 3:1 and the line intensities have been constrained to the ratios of 2:2:1. The parameters obtained from all three uranium spectra are shown in Table I. Dispersion effects<sup>33</sup> have been neglected in the data analysis since the transition energy falls below the  $K$ -x-ray absorption edge, and therefore are thought to be outside the accuracy of our measurement.

As may be seen from the data of Table I, the isomer shift  $\delta_{\text{IS}}$  of Eq. (2) has been experimentally determined within the limits of error for only the isotope  $^{234}\text{U}$ . The negative isomer shifts, Table I, indicate that the  $\gamma$ -ray transitions are more energetic in the sources used than in the absorber.

From Eq. (2) and a knowledge of  $\Delta|\psi(0)|^2$  between either of the two sources used and the  $(\text{UO}_2)_2\text{Rb}(\text{NO}_3)_3$  absorber we may evaluate  $\delta\langle r_n^2 \rangle$  for  $^{234}\text{U}$  and place an upper limit on  $\delta\langle r_n^2 \rangle$  for  $^{236}\text{U}$  and  $^{238}\text{U}$ . In order to estimate  $\Delta|\psi(0)|^2$ , calculations of the electronic charge density at the nucleus for several free-ion configurations of  $^{234}\text{U}$  and also  $^{237}\text{Np}$  have been made by means of a relativistic Hartree-Dirac wave-function code with Slater-Latter exchange.<sup>34</sup> These computations are summarized in Table II and changes in  $|\psi(0)|^2$  for these two isotopes are shown plotted as a function of the formal chemical oxidation state in Fig. 4. The various electronic configurations of  $^{234}\text{U}$  and  $^{237}\text{Np}$  were imposed upon the code in order of decreasing binding energy of the least tightly bound electrons. In every case between the +0 and +6 chemical oxidation state the least tightly bound electron is the same for Np and U since the 5*f* electrons are the most tightly bound. We find from our wave-function computations for all U isotopes that the removal of two 5*f*<sub>5/2</sub> electrons between +4 sources and +6 absorbers would produce an increase in the electron charge density at the origin of

$$\Delta|\psi(0)|^2 = 28.5 \times 10^{26} \text{ cm}^{-3},$$

due to the loss of screening of *s* electrons by these *f* electrons.

Assuming oxidation states of +4 for the  $\text{PuO}_2$  sources and +6 for the  $(\text{UO}_2)_2\text{Rb}(\text{NO}_3)_3$  absorbers the change in nuclear radius between the ground and excited states of the various U isotopes is given by

$$\frac{\delta\langle r_n^2 \rangle}{\langle r_n^2 \rangle} = \begin{cases} (-4.7 \pm 1.3) \times 10^{-6} & \text{for } ^{234}\text{U}, \\ (-11 \pm 11) \times 10^{-6} & \text{for } ^{236}\text{U}, \\ (-12 \pm 15) \times 10^{-6} & \text{for } ^{238}\text{U}. \end{cases}$$

The weakness of this argument lies in the uncertainty of the valence state of the  $\text{PuO}_2$  source and the  $(\text{UO}_2)_2\text{Rb}(\text{NO}_3)_3$  absorber, and for the metallic  $\text{PuAl}_4$  source there is an even less clear choice of oxidation state. We may, however, compare our measurements of isomer shift with the results

TABLE I. Measured Mössbauer parameters for (UO<sub>2</sub>)Rb(NO<sub>3</sub>)<sub>3</sub> absorbers at 4.2 °K.

Nucleus	Source material	Intensity (%) (Total for all three lines)	$\Gamma_{\text{exp}}$ FWHM <sup>a</sup> (mm/sec)	$\frac{3}{8}eqQ$ (mm/sec)	$\delta_{\text{IS}}$ (mm/sec) <sup>b</sup>
<sup>234</sup> U	PuAl <sub>4</sub>	3.4	36.5 ± 0.3	-60.1 ± 0.3	-1.6 ± 0.2
<sup>234</sup> U	PuO <sub>2</sub>	3.4	48.3 ± 0.4	-58.8 ± 0.3	-0.7 ± 0.2
<sup>236</sup> U	PuO <sub>2</sub>	1.4	46.2 ± 2.6	-58.1 ± 2.6	-1.6 ± 1.6
<sup>238</sup> U	PuO <sub>2</sub>	6.1	48.6 ± 3.8	-65.4 ± 3.9	-1.8 ± 2.2

<sup>a</sup>Full width at half-maximum.<sup>b</sup>Estimated systematic errors have been included in the data.

for similar <sup>237</sup>Np compounds and alloys, if we assume a similar electronic response to a changing chemical environment for these two neighboring elements in the Periodic Table. In drawing such a correlation between the isomer shifts we assume that the additional 5f<sub>5/2</sub> electron of Np in these substances has at most a linear effect upon changes of  $|\psi(0)|^2$  brought about by changes in the chemical oxidation state. Support of this contention is seen in the computational analysis shown in Fig. 4. The existence of the extra 5f<sub>5/2</sub> electron for the Np ions and the larger central attractive charge of the Np nucleus causes on the average a 9% larger change in  $|\psi(0)|^2_{\text{Np}}$  than for corresponding oxidation states of U, but aside from this scaling the shapes are similar.

One isomer-shift study of <sup>237</sup>Np compounds has shown that effects of covalency are smaller than changes in formal chemical oxidation state.<sup>35</sup> A more recent study by Dunlap *et al.*<sup>36</sup> which compares neptunium fluoride absorbers to (NpO<sub>2</sub>)Rb(NO<sub>3</sub>)<sub>3</sub> indicates a much lower oxidation state of ~+5.1 for this compound and hence suggests a stronger covalency effect.

We show in Fig. 5 how isomer shifts between similar source materials and similar absorber materials for the <sup>237</sup>Np and <sup>234</sup>U isotopes compare. The least-squares fit of a straight line, passing through the origin, to the data of Fig. 5 yields (in energy units)

$$\delta_{\text{IS, U}} = (\pm 0.030 \pm 0.013)\delta_{\text{IS, Np}}(E_{\gamma, \text{U}}/E_{\gamma, \text{Np}}),$$

and from Eq. (2) we see that

$$(\delta\langle r_n^2 \rangle / \langle r_n^2 \rangle)_{\text{U}} = (0.025 \pm 0.011)(\delta\langle r_n^2 \rangle / \langle r_n^2 \rangle)_{\text{Np}},$$

where we have used the values  $\Delta|\psi(0)|^2_{\text{Np}}/\Delta|\psi(0)|^2_{\text{U}} = 1.09$ ,  $E_{\gamma, \text{U}}/E_{\gamma, \text{Np}} = 0.73$ ,  $Z_{\text{Np}}/Z_{\text{U}} = 1.01$ , and  $\langle r_n^2 \rangle_{\text{Np}}/\langle r_n^2 \rangle_{\text{U}} = 1.01$ . Using the results of Dunlap *et al.*<sup>36</sup> for  $(\delta\langle r_n^2 \rangle)_{\text{Np}} = (-27 \pm 5) \times 10^{-3} \text{ fm}^2$  and  $\langle r_n^2 \rangle = (1.2A^{1/3} \text{ fm})^2$  we conclude that

$$\delta\langle r_n^2 \rangle / \langle r_n^2 \rangle = (-12.2 \pm 5.9) \times 10^{-6} \text{ for } ^{234}\text{U}.$$

This value is larger in magnitude than the previously determined value from the PuO<sub>2</sub> source alone in part because of the smaller estimate of  $\Delta|\psi(0)|^2_{\text{Np}}$  used by Dunlap *et al.* as suggested by the fluoride results. The value is also influenced

TABLE II. Relativistic values of the electronic probability density at the origin for <sup>234</sup>U and <sup>237</sup>Np.

Oxidation state	<sup>234</sup> U configuration (In addition to the Radon core)	<sup>237</sup> Np configuration (In addition to the Radon core)	$ \psi(0) ^2_{\text{U}}$ (10 <sup>7</sup> a. u. <sup>a,b</sup> )	$ \psi(0) ^2_{\text{Np}}$ (10 <sup>7</sup> a. u. <sup>a,c</sup> )
(0)	7s <sup>2</sup> 6d <sup>1</sup> 5f <sup>6</sup>	7s <sup>2</sup> 6d <sup>1</sup> 5f <sup>4</sup>	7.88930	8.57385
(I)	7s <sup>2</sup> 5f <sup>3</sup>	7s <sup>2</sup> 5f <sup>4</sup>	7.88944	8.57400
(II)	7s <sup>1</sup> 5f <sup>3</sup>	7s <sup>1</sup> 5f <sup>4</sup>	7.88923	8.57377
(III)	5f <sup>3</sup>	5f <sup>4</sup>	7.88897	8.57348
(IV)	5f <sup>2</sup>	5f <sup>3</sup>	7.88919	8.57372
(V)	5f <sup>1</sup>	5f <sup>2</sup>	7.88944	8.57399
(VI)		5f <sup>1</sup>	7.88972	8.57430
(VII)				8.57463

<sup>a</sup>One a. u. is equal to 0.538 × 10<sup>24</sup> cm<sup>-3</sup> = 1/(4πa<sub>0</sub><sup>3</sup>).<sup>b</sup>The "equivalent" radius of the uniformly charged U nucleus was 6.7675 × 10<sup>-13</sup> cm.<sup>c</sup>The equivalent radius of the uniformly charged Np nucleus was 6.7963 × 10<sup>-13</sup> cm.

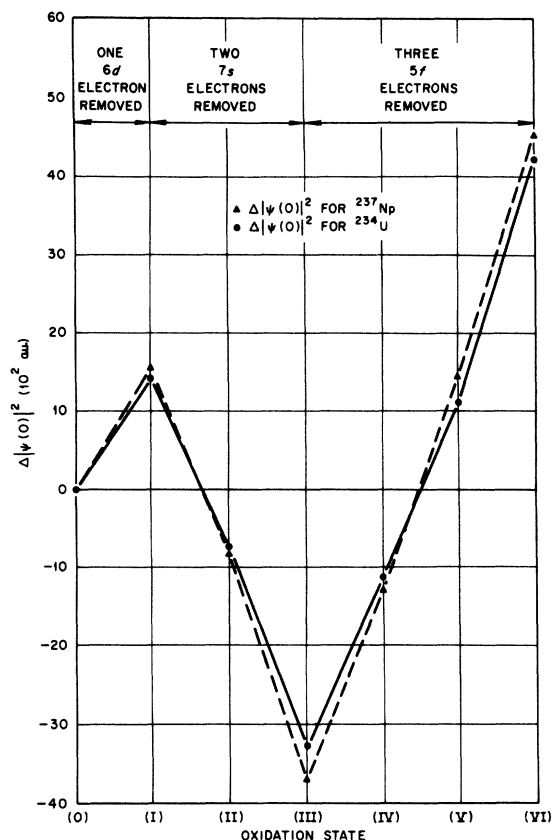


FIG. 4. Changes in the relativistic electron probability density at the origin with chemical oxidation state for  $^{234}\text{U}$  and  $^{237}\text{Np}$ . One a. u. is equal to  $0.538 \times 10^{24} \text{ cm}^{-3} = 1/(4\pi a_0^3)$ .

by the relatively larger measured isomer shift (Fig. 5) for the  $\text{PuAl}_4$  source. We favor this larger number due to the increased information used in its computation.

A similar computation for the other isotopes gives

$$\frac{\delta \langle r_n^2 \rangle}{\langle r_n^2 \rangle} = \begin{cases} (-21 \pm 21) \times 10^{-6} & \text{for } ^{236}\text{U}, \\ (-23 \pm 28) \times 10^{-6} & \text{for } ^{238}\text{U}. \end{cases}$$

These values are substantially below a theoretical value of  $+31.2 \times 10^{-6}$  for the  $^{234}\text{U}$  nucleus which was calculated by Marshalek<sup>37</sup> using a self-consistent cranking model with Coriolis antipairing and centrifugal stretching of the nucleus. More importantly the sign of  $\delta \langle r_n^2 \rangle / \langle r_n^2 \rangle$  is negative and hence indicates a shrinking of the nucleus in the transition from its  $0^+$  ground state to its  $2^+$  first excited state. However, Meyer and Speth<sup>38</sup> show that a more dominant role for the Coriolis antipairing effect occurs in a second-order cranking model. This term leads to shrinking of charge

radii for many deformed nuclei in the region below Pb but calculations have not been made for the actinides.

The ratios of the quadrupole moments of the three isotopes may be determined from the quadrupole coupling constants ( $\frac{2}{3}eqQ$ ) listed in Table I. Since the same absorber material was used in each experiment,  $q$  may be assumed to be a constant. For the  $\text{PuO}_2$  data this gives the ratios

$$Q_{236}/Q_{234} = 0.99 \pm 0.05, \quad Q_{238}/Q_{234} = 1.11 \pm 0.07.$$

These values agree fairly well with others recently determined by Mössbauer measurements<sup>39</sup> and from  $B(E2)$  values.<sup>28</sup> The ratios differ slightly from those previously reported by the authors<sup>40,41</sup> due to the fact that the full transmission integral was used to fit the data reported here instead of the Lorentzian approximation, which was used in our earlier analysis.

Since the spectra were asymmetric, both the magnitude and the sign of the quadrupole coupling constant can be determined. The intrinsic quadrupole moment of the  $^{234}\text{U}$  nucleus is known from  $B(E2)$  values<sup>28</sup> to be  $Q_0 = (10.19 \pm 0.13) \times 10^{-24} \text{ cm}^2$ .

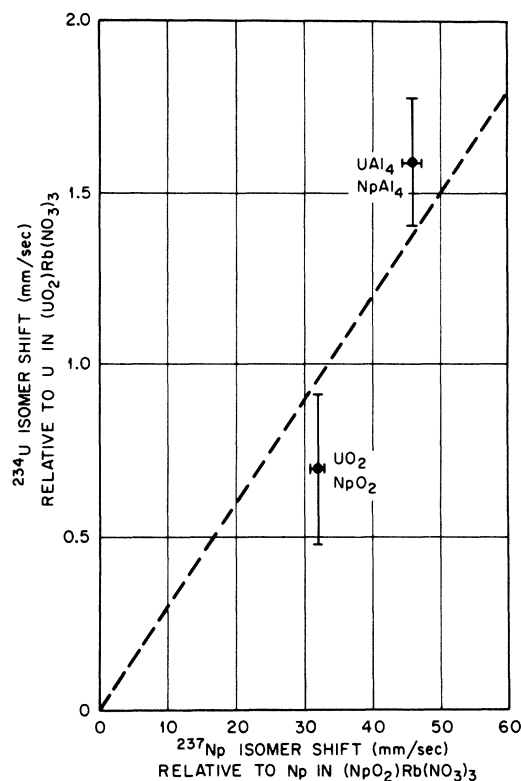


FIG. 5. Mössbauer isomer shift of the 43.5-keV  $\gamma$  ray of  $^{234}\text{U}$  and  $\text{UAl}_4$  and  $\text{UO}_2$  relative to  $(\text{UO}_2)\text{Rb}(\text{NO}_3)_3$  vs the Mössbauer isomer shift of the 59.6-keV  $\gamma$  ray of  $^{237}\text{Np}$  in  $\text{NpAl}_4$  and  $\text{NpO}_2$  relative to  $(\text{NpO}_2)\text{Rb}(\text{NO}_3)_3$  at 4.2°K. The straight line is a least-squares fit to the data.

The spectroscopic quadrupole moment in the strong coupling model is given by

$$Q(I, M, K) = Q_0 \frac{[3M^2 - I(I+1)][3K^2 - I(I+1)]}{I(I+1)(2I-1)(2K+3)} \quad (6)$$

Thus,

$$Q = Q(2, 2, 0) = -\frac{2}{7}Q_0 = (-2.91 \pm 0.04) \times 10^{-24} \text{ cm}^2$$

for the  $^{234}\text{U}$  nucleus. Using the value  $\frac{3}{8}eQq = (-60.1 \pm 0.3) \text{ mm/sec}$  (Table I) one obtains  $q = (8.14 \pm 0.13) \times 10^{18} \text{ V/cm}^2$ . This negative electric field gradient at the uranium nucleus which is directed parallel to the crystalline  $c$  axis (the O-U-O axis) is evidence that the bonding produces a concentration of electronic charge in the  $x$ - $y$  plane in confirmation of results from previous nuclear orientation studies.<sup>20</sup>

Lattice parameters of Pu compounds have been reported<sup>42</sup> to increase continuously with time when the compounds were kept sealed at room temperature. This increase might be thought of as due to the displacement of atoms to interstitial sites by the recoil from  $\alpha$  emission. It has been estimated<sup>43</sup>

that as many as 1500 of these defects (Frenkel pairs) are produced per  $\alpha$  disintegration for  $\text{PuO}_2$  and that the exponential-growth time constant for the resulting lattice parameter is 3.68 days. The resulting saturation concentration of Frenkel defects would be one-half to one defect pair per unit cell and would possibly lead to distributions of electric field gradients at the Pu site. These effects could lead to quadrupole interactions in the  $\text{PuO}_2$  sources and produce asymmetric broadening of the spectral lines. Lattice parameters of PuAl alloys have also been found<sup>44</sup> to increase after a 10-yr storage at room temperature. Self-irradiation damage and subsequent annealing in the PuAl alloys might however be expected to produce a lower saturation concentration in this intermetallic compound than in the insulator  $\text{PuO}_2$ .

Such effects (if present) have not been observed to significantly change the Mössbauer absorption lines with time. Successive spectra were analyzed for such broadening effects after sources were kept four months at room temperature and after four days at 4.2 °K with statistically insignificant results.

†(Research jointly sponsored by the University of Tennessee and the U. S. Atomic Energy Commission under contract with the Union Carbide Corporation.)

\*National Science Foundation Fellow. Research done in partial fulfillment of the requirements for the Ph. D. degree at the University of Tennessee. Present address: Lawrence Berkeley Laboratories, Berkeley, Calif. 94720.

<sup>1</sup>J. A. Stone, International Atomic Energy Agency Technical Report Series No. 50, 1966, p. 174 (unpublished).

<sup>2</sup>P. Kienle, in *Hyperfine Structure and Nuclear Radiations*, edited by E. Matthias and D. A. Shirley (North-Holland, Amsterdam, 1968), p. 27.

<sup>3</sup>J. R. Oleson, Y. K. Lee, J. C. Walker, and J. W. Wiggins, *Phys. Lett. B* **25**, 258 (1967).

<sup>4</sup>N. Hershkowitz, C. G. Jacobs, Jr., and K. A. Murphy, *Phys. Lett.* **27**, 563 (1968).

<sup>5</sup>J. A. Stone and W. L. Pillinger, *Phys. Rev. Lett.* **13**, 200 (1964).

<sup>6</sup>J. G. Mullen, *Phys. Lett.* **15**, 15 (1965).

<sup>7</sup>S. L. Ruby, G. M. Kalvius, B. D. Dunlap, G. K. Shenoy, D. Cohen, M. B. Brodsky, and D. J. Lam, *Phys. Rev.* **184**, 374 (1969).

<sup>8</sup>G. K. Shenoy, G. M. Kalvius, S. L. Ruby, B. D. Dunlap, Moshe Kuznietz, and F. P. Campos, *Int. J. Magn.* **1**, 23 (1970).

<sup>9</sup>C. M. Lederer, J. M. Hollander, and I. Perlman, *Table of Isotopes* (Wiley, New York, 1967).

<sup>10</sup>M. Schmorak, C. E. Bemis, Jr., M. J. Zender, N. B. Gove, and P. F. Dittner, *Nucl. Phys. A* **178**, 410 (1972).

<sup>11</sup>W. H. Zachariasen, *Acta Crystallogr.* **2**, 388 (1949).

<sup>12</sup>G. Raphael and R. Lallement, *Solid State Commun.* **6**, 383 (1968).

<sup>13</sup>F. S. Galasso, *Structure and Properties of Inorganic Solids* (Pergamon, Oxford, England, 1970).

<sup>14</sup>B. S. Borie, Jr., *Trans. AIME (Am. Inst. Min. Metal. Pet. Eng.)* **191**, 800 (1951).

<sup>15</sup>O. J. C. Runnalls, in *Plutonium* 1965, edited by A. E. Kay and M. B. Waldron (Chapman and Hall, London, 1967), p. 341.

<sup>16</sup>M. C. Gregory, R. W. Longheed, and E. K. Hulet, *Bull. Am. Phys. Soc.* **17**, 546 (1962); M. C. Gregory (private communication).

<sup>17</sup>W. D. Durbh, J. E. Bigelow, and L. J. King, Oak Ridge National Laboratory Report No. 4718, 1971, p. 21 (unpublished).

<sup>18</sup>J. W. T. Dabbs, L. D. Roberts, and G. W. Parker, *Physica (Utr.)* **24**, S69 (1958).

<sup>19</sup>L. D. Roberts, J. W. T. Dabbs, and G. W. Parker, *Proc. 2nd UN Int. Conf. PUAE* **15**, 322 (1958).

<sup>20</sup>L. D. Roberts, J. W. T. Dabbs, F. J. Walter, S. H. Hanauer, and G. W. Parker, *Radioisotopes in the Physical Sciences and Industry*, (International Atomic Energy Agency, Vienna, 1962), Vol. 1, p. 329.

<sup>21</sup>J. L. Hoard and J. P. Stroupe, USAEC TID Report No. 5290, 1958, p. 323 (unpublished).

<sup>22</sup>J. I. Bullock, *J. Chem. Soc. (Lond.) A* **5**, 781 (1969).

<sup>23</sup>G. A. Barclay, T. M. Sabine, and J. C. Taylor, *Acta Crystallogr.* **19**, 205 (1965).

<sup>24</sup>D. A. Shirley, *Rev. Mod. Phys.* **36**, 339 (1964).

<sup>25</sup>B. Friche and J. T. Waber, *Phys. Rev. B* **5**, 3445 (1972).

<sup>26</sup>J. L. C. Ford, Jr., P. H. Stelson, C. E. Bemis, Jr., F. K. McGowan, R. L. Robinson, and W. T. Milner, *Phys. Rev. Lett.* **27**, 1232 (1971).

<sup>27</sup>A. Bohr and V. F. Weisskopf, *Phys. Rev.* **77**, 94 (1950).

<sup>28</sup>S. G. Nilsson, C. F. Tsang, A. Sobiczewski, Z. Szymanski, S. Wycech, C. Gustafson, I. Lamm, P. Möller, and B. Nilsson, *Nucl. Phys. A* **131**, 1 (1969).

<sup>29</sup>C. E. Bemis, Jr., F. K. McGowan, J. L. C. Ford,

- Jr., W. T. Milner, P. H. Stelson, and R. L. Robinson, Phys. Rev. C 8, 1466 (1973).
- <sup>30</sup>G. H. Dieke and A. B. F. Duncan, *Spectroscopic Properties of Uranium Compounds* (McGraw-Hill, New York, 1949), p. 15.
- <sup>31</sup>J. C. Waldron, Atomic Energy Research Establishment HARWELL, Report No. AERE-R6141, 1969 (unpublished).
- <sup>32</sup>A. I. Komyak, Vestn. Akad. Nauk. SSR, Ser. Fiz.-Mat. Nauk. No. 2, 85 (1969).
- <sup>33</sup>F. E. Wagner, B. D. Dunlap, G. M. Kalvius, H. Schaller, R. Felscher, and H. Spieler, Phys. Rev. Lett. 28, 530 (1972).
- <sup>34</sup>T. C. Tucker, L. D. Roberts, C. W. Nestor, Jr., T. A. Carlson, and F. B. Malik, Phys. Rev. 178, 998 (1969).
- <sup>35</sup>J. A. Stone, W. L. Pillinger, and D. G. Karraker, Inorg. Chem. 8, 2519 (1969).
- <sup>36</sup>B. D. Dunlap, G. K. Shenoy, G. M. Kalvius, and D. Cohen, *Hyperfine Interactions in Excited Nuclei*, edited by G. Goldring and R. Kalish (Gordon and Breach, New York, 1972).
- <sup>37</sup>E. R. Marshalek, Phys. Rev. Lett. 20, 214 (1968).
- <sup>38</sup>J. Meyer and J. Speth, Nucl. Phys. A 203, 17-41 (1973).
- <sup>39</sup>R. Meeker, G. M. Kalvius, B. D. Dunlap, S. L. Ruby, and D. Cohen, Bull. Am. Phys. Soc. 17, 85 (1972).
- <sup>40</sup>J. A. Monard, Paul G. Huray, and J. O. Thomson, Bull. Am. Phys. Soc. 17, 86 (1972).
- <sup>41</sup>Paul G. Huray, J. A. Monard, and J. O. Thomson, Oak Ridge National Laboratory Report No. 4743, 1972, p. 100 (unpublished).
- <sup>42</sup>M. H. Rand, A. C. Fox, and R. S. Street, Nature 195, 567 (1962).
- <sup>43</sup>G. M. Kinchin and R. S. Pease, Rep. Prog. Phys. 18, 1 (1955).
- <sup>44</sup>F. H. Ellinger, C. C. Land, and W. N. Miner, J. Nucl. Mater. 5, 165 (1962).



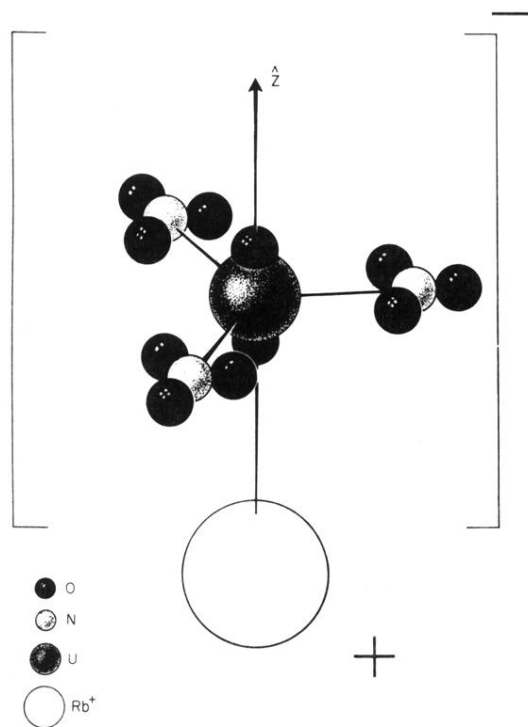


FIG. 1. Structure of the uranyl rubidium nitrate molecule. The three nitrate groups are shown lying in a plane perpendicular to the collinear O-U-O entity.